

## ANALYTICAL SOLUTIONS OF FRACTAL-HYDRO-THERMAL MODEL FOR TWO-PHASE FLOW IN THERMAL STIMULATION ENHANCED COALBED METHANE RECOVERY

by

**Xiaoji SHANG<sup>a</sup>, Jianguo WANG<sup>b\*</sup>, and Zhizhen ZHANG<sup>b</sup>**

<sup>a</sup> State Key Laboratory for GeoMechanics and Deep Underground Engineering,  
China University of Mining and Technology, Xuzhou, China

<sup>b</sup> School of Mechanics and Civil Engineering, China University of Mining and Technology,  
Xuzhou, China

Original scientific paper  
<https://doi.org/10.2298/TSCI180620132S>

*Thermal stimulation is a useful supplementary mining technique for the enhancement of coalbed methane recovery. This technique couples the temperature change with gas-water two-phase flow in the mining process. Many integer dimension hydro-thermal models have been proposed but cannot well describe this coupling because two-phase flow and heat conduction are usually non-linear, tortuous and fractal. In this study, a fractal-hydro-thermal coupling model is proposed to describe the coupling between heat conduction and two-phase flow behaviors in terms of fractional time and space derivatives. This model is analytically solved through the fractal travelling-wave method for pore pressure and production rate of gas and water. The analytical solutions are compared with the in-situ coalbed methane production rate. Results show that our proposed fractal-hydro-thermal model can describe both heat and mass transfers in thermal stimulation enhanced coalbed methane recovery.*

Key words: *heat conduction, two-phase flow, hydro-thermal coupling model, fractal travelling-wave method, local fractional operator*

### Introduction

Thermal stimulation is a useful supplementary mining technique for the enhancement of coalbed methane (CBM) recovery [1]. In this technique, hot water [2] or hot gas [3, 4] is injected to induce the thermal effect on gas production. In the process of these thermal stimulations, temperature and seepage fields co-exist in the coal seam, and gas-water two-phase flow and temperature complexly interact. Theoretical and numerical simulations have been conducted to establish a mathematical model for the coupling of heat conduction and two-phase flow along the flow path [5]. Two-phase flow models [6, 7], hydro-thermal coupling models [8, 9], thermal-hydro-mechanical (THM) coupling models [10], and THM coupling model with two-phase flow [11] have been proposed so far. For example, Teng *et al.* [10] proposed a fully coupled THM model to quantitatively predict the heat and mass transfers in thermal stimulation enhanced coal seam gas recovery. This model only considered one-phase flow. Taking the effects of temperature and groundwater into account, Li *et al.* [11] developed a fully coupled THM model for two-phase flow in CBM extraction. However, these models did not consider

\* Corresponding author, e-mail: [jgwang@cumt.edu.cn](mailto:jgwang@cumt.edu.cn); [nuswjg@yahoo.com](mailto:nuswjg@yahoo.com)

the heterogeneous pores and tortuous fractures in the real coal seam structure and no analytical solutions of gas production rate in the THM models have been obtained.

The gas-water two-phase flow in porous rock matrix is usually non-linear, tortuous and fractal. An anomalous two-phase flow rather than Darcy flow may dominate the process of thermal stimulation enhanced CBM recovery [12]. In addition, the pathway of heat conduction is also anomalous. The effects of these anomalous mass and heat transfer on the process of thermal stimulation enhanced CBM recovery should be studied. A fractional derivative model is a good option for the simulation of real two-phase flow and heat conduction. The theory of local fractional derivatives has been successfully applied to many problems in fluid mechanics [13, 14]. The fractal travelling-wave method was introduced to solve these local fractional models [15]. A local fractional heat conduction equation has been solved by the local variational iteration method [9]. However, two-phase flow problems in heat transfer process are still not studied.

The literatures review reveals two imperfections. The first is that previous studies have not involved the coupling between the fractal gas-water two-phase flow and heat conduction. The second is that analytical solutions for the coupled thermal-hydro model are scarce in thermal stimulation enhanced CBM recovery. This study is to improve these two imperfections with following approach. Firstly, a fractal-thermal two-phase flow coupling model is proposed to describe the two-phase flow behaviors in heat transfer process. Secondly, this set of coupling equations is solved through travelling-wave method. The fractal analytical solutions for gas pressure and gas production rate, water pressure and water production rate are then obtained. The water and gas production rate are validated by in-situ production data [11, 16], respectively. Finally, the conclusions are made.

### Mathematical formulation of thermal-hydro coupling model

A fully coupled thermal-hydro model to couple the governing equations between gas-water two-phase flow and heat conduction is established based on following assumptions:

- fractured coal is a heterogeneous, anisotropic, rigorous, and porous continuum,
- coal seam gas is ideal, and its viscosity does not change with temperature, and
- gas seepage obeys fractal Darcy's law.

#### Governing equation for fractal heat conduction

In fractal porous media, heat conduction obeys the energy conservation law in fractal form [9]:

- for gas phase

$$\frac{C_{eq,g} \partial^\alpha [T_g(x,t)]}{\partial t^\alpha} - K_{eq,g} \frac{\partial^{2\alpha} [T_g(x,t)]}{\partial x^{2\alpha}} = Q_T \quad (1)$$

- for water phase

$$\frac{C_{eq,g} \partial^\alpha [T_w(x,t)]}{\partial t^\alpha} - K_{eq,g} \frac{\partial^{2\alpha} [T_w(x,t)]}{\partial x^{2\alpha}} = Q_T \quad (2)$$

where the space local fractional derivative of fractal order  $\alpha$  is  $\nabla^\alpha = \partial/\partial x^\alpha$  and  $0 < \alpha \leq 1$ ,  $C_{eq,g}$  and  $C_{eq,w}$  are the specific heat capacity of gas and water, respectively. The  $T_g$  and  $T_w$  – the temperature of gas and water, respectively,  $K_{eq,g}$  and  $K_{eq,w}$  – the effective thermal conductivity of gas and water, respectively,  $t$  – the time, and  $Q_T$  – the heat source.

*Continuity equations for fractal two-phase flow*

– for gas phase

$$\frac{\partial^\alpha [\phi s_g \rho_g(x,t)]}{\partial t^\alpha} + \nabla^\alpha [\rho_g(x,t) v_g(x,t)] = Q_g \tag{3}$$

– for water phase

$$\frac{\partial^\alpha (\phi s_w \rho_w)}{\partial t^\alpha} + \nabla^\alpha [\rho_w v_w(x,t)] = Q_w \tag{4}$$

Since water is slightly compressible, its density  $\rho_w$  can be regarded as a constant. The gas density,  $\rho_g$ , follows the equation of state:

$$\rho_g = \frac{M}{ZRT_g} p_g \tag{5}$$

where  $\phi$  is the coal porosity,  $\rho_w$  and  $\rho_g$  are the water and gas density under formation conditions, respectively. The  $Q_g$  and  $Q_w$  – the source strength of gas and water, respectively,  $s_g$  and  $s_w$  – the saturation of gas and water, and  $s_g + s_w = 1$ . The  $M$  is the gas molecular weight,  $Z$  – the gas compressibility factor, and  $R$  – the universal gas constant.

*Fractional Darcy velocity for fractal two-phase flow*

The real flow pathway of fluid is along the tortuous fractures of rock. Hence, the flow is fractal and the fractional Darcy velocity of fluid without gravity effect [6, 13]:

$$\phi s_g v_g = -\frac{kk_{rg}}{\mu_g} \nabla^\alpha p_g \tag{6}$$

$$\phi s_w v_w = -\frac{kk_{rw}}{\mu_w} \nabla^\alpha p_w \tag{7}$$

where  $v_g$  and  $v_w$  are the velocity of gas and water, respectively,  $k$  – the absolute permeability,  $k_{rg}$  and  $k_{rw}$  are the relative permeability of gas and water, respectively,  $\mu_g$  and  $\mu_w$  – the viscosity of gas and water, respectively,  $p_g$  and  $p_w$  – the pressure of gas and water, respectively.

Integrating eqs. (6) and (7) into eq. (3) yields the governing equation for gas-flow in a fractal porous medium:

$$\frac{p_g M}{ZRT_g} S \frac{\partial^\alpha p_g}{\partial t^\alpha} + \nabla^\alpha \left( \frac{p_g M}{ZRT_g} \left( -\frac{kk_{rg}}{\mu_g} \nabla^\alpha p_g \right) \right) = Q_g \tag{8}$$

where  $S$  is the storage coefficient of CBM [17]:

$$S = \left( \frac{\phi s_g}{\rho_g} \right) \left( \frac{\partial \rho_g}{\partial p_g} \right) + \frac{\partial (\phi s_g)}{\partial p_g} \tag{9}$$

Integrating eq. (7) into eq. (4) yields the governing equation for water flow:

$$\nabla^\alpha \left( -\frac{kk_{rw}}{\mu_w} \nabla^\alpha p_w \right) = Q_w \tag{10}$$

**Travelling-wave transformation**

In this section, we find the travelling-wave solutions of the previously-developed PDE for temperature, gas, and water pressures. The travelling-wave transformation of the non-differentiable type,  $c$  is a constant [9]:

$$\theta^\alpha = x^\alpha - ct^\alpha \quad (11)$$

Thus, we have the function  $p_g(\theta) = p_g(x, t)$  such that:

$$\frac{\partial^\alpha p_g(x, t)}{\partial x^\alpha} = \frac{\partial^\alpha p_g}{\partial \theta^\alpha} \left( \frac{\partial \theta}{\partial x} \right)^\alpha = \frac{\partial^\alpha p_g}{\partial \theta^\alpha}, \quad \frac{\partial^{2\alpha} p_g(x, t)}{\partial x^{2\alpha}} = \frac{\partial^{2\alpha} p_g}{\partial \theta^{2\alpha}} \quad (12)$$

and

$$\frac{\partial^\alpha p_g(x, t)}{\partial t^\alpha} = \frac{\partial^\alpha p_g}{\partial \theta^\alpha} \left( \frac{\partial \theta}{\partial t} \right)^\alpha = -c \frac{\partial^\alpha p_g}{\partial \theta^\alpha} \quad (13)$$

Similarly, we have the function  $T(\theta) = T(x, t)$  such that:

$$\frac{\partial^\alpha T(x, t)}{\partial t^\alpha} = \frac{\partial^\alpha T}{\partial \theta^\alpha} \left( \frac{\partial \theta}{\partial t} \right)^\alpha = -c \frac{\partial^\alpha T}{\partial \theta^\alpha} \quad (14)$$

#### Analytical solutions for temperature

For the convenience of calculation, eq. (1) is simplified into:

$$\frac{C_{\text{eq},g}}{K_{\text{eq},g}} \frac{\partial^\alpha [T_g(x, t)]}{\partial t^\alpha} - \frac{\partial^{2\alpha} [T_g(x, t)]}{\partial x^{2\alpha}} = 0 \quad (15)$$

For gas phase, the solution of temperature is obtained [9]:

$$T_g(x, t) = \gamma_{T_0} E_\alpha \left( -\frac{C_{\text{eq},g}}{K_{\text{eq},g}} c \theta^\alpha \right) \quad (16)$$

where  $\gamma_{T_0}$  is a constant which is  $\gamma_{T_0} = \gamma_T T_0$ .

The Mittag-Leffler function on fractal sets is defined [13]:

$$E_\alpha(\theta^\alpha) = \sum_{i=0}^{\infty} \frac{\theta^{i\alpha}}{\Gamma(1+i\alpha)} \quad (17)$$

For water phase, the solution of temperature is similarly obtained [9]

$$T_w(x, t) = \gamma_{T_0} E_\alpha \left( -\frac{C_{\text{eq},w}}{K_{\text{eq},w}} c \theta^\alpha \right) \quad (18)$$

#### Analytical solutions for gas phase pressure and water pressure

Substituting eqs. (12) and (13) into eq. (8) gets the governing equation for gas-flow:

$$\frac{-p_g McS}{ZRT_g} \frac{\partial^\alpha p_g}{\partial \theta^\alpha} + \frac{\partial^\alpha}{\partial \theta^\alpha} \left[ \frac{p_g M}{ZRT_g} \left( -\frac{kk_{rg}}{\mu_g} \frac{\partial^\alpha p_g}{\partial \theta^\alpha} \right) \right] = Q_g \quad (19)$$

Equation can be re-written:

$$-cSU + \frac{\partial^\alpha}{\partial \theta^\alpha} \left( -\frac{kk_{rg}}{\mu_g} U \right) = Q_g \quad \text{and} \quad U(\theta) = \frac{p_g M}{ZRT_g} \frac{\partial^\alpha p_g}{\partial \theta^\alpha} \quad (20)$$

Following the idea [15], we set the form of the solution:

$$U(\theta) = \gamma_{p_g^0} E_\alpha(\chi \theta^\alpha) \quad (21)$$

$$\frac{d^\alpha U(\theta)}{d\theta^\alpha} = \frac{d^\alpha}{d\theta^\alpha} [\gamma_{p_0} E_\alpha(\chi\theta^\alpha)] = \gamma_{p_0} \chi E_\alpha(\chi\theta^\alpha) \quad (22)$$

where  $\gamma_{T_0}$  and  $\chi$  are constants. Similarly,  $\gamma_{p_0}$  is expressed as  $\gamma_{p_0} = \gamma_p p_0$ .

Therefore,

$$-Sc\gamma E_\alpha(\chi\theta^\alpha) - \frac{kk_{rg}}{\mu_g} \gamma_{p_0} \chi E_\alpha(\chi\theta^\alpha) = 0, \text{ or } -Sc - \frac{kk_{rg}}{\mu_g} \chi = 0 \quad (23)$$

Making use of eqs. (20) and (23) obtains the travelling-wave solution for gas pressure:

$$U(x, t) = \gamma_{p_0} E_\alpha\left(-\frac{\mu_g Sc}{kk_{rg}} \theta^\alpha\right) \quad (24)$$

Integrating eqs. (16) and (24) into eq. (20) yields:

$$\frac{p_g \partial^\alpha p_g}{\partial \theta^\alpha} = \frac{ZR\gamma_{T_0}\gamma_{p_0}}{M} E_\alpha\left(-\frac{C_{eq,g}c}{K_{eq,g}} \theta^\alpha\right) E_\alpha\left(-\frac{\mu_g Sc}{kk_{rg}} \theta^\alpha\right) \quad (25)$$

Equation (25) can be translated into [13]:

$$\frac{\partial^\alpha \left(\frac{p_g^2}{2}\right)}{\partial \theta^\alpha} = \frac{ZR\gamma_{T_0}\gamma_{p_0}}{M} E_\alpha\left[-\left(\frac{C_{eq,g}c}{K_{eq,g}} + \frac{\mu_g Sc}{kk_{rg}}\right) \theta^\alpha\right] \quad (26)$$

The local fractional integral of  $f(x)$  is defined [13]:

$${}_a I_x^{(\alpha)} f(x) = \frac{1}{\Gamma(1+\alpha)} \int_a^x f(s) (ds)^\alpha, \quad 0 \leq \alpha < 1 \quad (27)$$

Integrating eq. (27) into eq. (26) yields the fractional analytical solution of gas pressure:

$$p_g = \sqrt{\frac{ZR\gamma_{T_0}\gamma_{p_0}}{M} E_\alpha\left[-\left(\frac{C_{eq,g}c}{K_{eq,g}} + \frac{\mu_g Sc}{kk_{rg}}\right) \frac{\theta^{2\alpha}}{\Gamma(1+\alpha)}\right]} \quad (28)$$

For water phase, the fractional analytical solution of water phase pressure is obtained:

$$p_w = \frac{Q_w \mu_w}{kk_{rw}} \frac{\theta^{2\alpha}}{2\Gamma^2(1+\alpha)} \quad (29)$$

### Analytical solution of gas and water production rate

Being similar form to the CBM production rate in normal space yields the gas and water production rate [18]:

$$\frac{d^\alpha [G_{p_g}(t)]}{dt^\alpha} = -\int_\Omega \left(\frac{\phi}{p_a} \frac{d^\alpha p_g}{dt^\alpha}\right) dv \quad \text{and} \quad \frac{d^\alpha [G_{p_w}(t)]}{dt^\alpha} = -\int_\Omega \left(\frac{\phi}{p_a} \frac{d^\alpha p_w}{dt^\alpha}\right) dv \quad (30)$$

where the atmospheric pressure  $p_a = 101.3$  kPa.

### Model verifications with gas production rate

The fractal analytical solutions of gas and water production rates were compared with the recorded production rates of No. 1 CBM well in southern district of Fanzhuang block [11], respectively. The parameters taken from Li *et al.* [11] are listed in tab. 1 for calculation.

**Table 1. Model parameters in calculation for No. 1 CBM well**

Parameter	Unit	Value	Physical meanings
$C_{eq,g}$	$[JK^{-1}kg^{-1}]$	2160	Specific heat capacity of gas
$C_{eq,w}$	$[JK^{-1}kg^{-1}]$	4200	Specific heat capacity of water
$K_{eq,g}$	$[Wm^{-1}K^{-1}]$	0.031	Thermal conductivity of gas
$K_{eq,w}$	$[Wm^{-1}K^{-1}]$	0.598	Thermal conductivity of water
$\mu_w$	$[Pa \cdot s]$	$1.01 \cdot 10^{-3}$	Water viscosity
$\mu_g$	$[Pa \cdot s]$	$1.84 \cdot 10^{-5}$	Gas viscosity
$\phi$		0.01	Porosity
$c$	$[ms^{-1}]$	$6 \cdot 10^{-1}$	Travel wave viscosity
$\alpha$		0.35	Fractal order
$\gamma_{T_0}$		0.002	Coefficient of temperature
$T_0$	$[K]$	312.5	Initial injection temperature
$\gamma_{P_0}$		0.14	Coefficient of pressure
$p_0$	$[MPa]$	5.24	Initial average pressure
$k_0$	$[mD]$	0.5	Initial permeability in fractured zone
$k_{rw}$		1	Relative permeability for water
$k_{rg}$		0.756	Relative permeability for gas
$S$		$5 \cdot 10^{-6}$	Storage coefficient of gas
$Z$		1	Gas compressibility factor
$R$	$[Jmol^{-1}K^{-1}]$	8.314	Universal gas constant
$M$		16.0425	Molecular weight of gas

Both gas and water production rates from the No. 1 CBM well [11] are used to verify the fractal analytical solutions. The gas production rate is shown in fig. 1(a) and the water production rate is compared in fig. 1(b). As shown, the gas production rate of No. 1 CBM well firstly increases and then gradually decreases with time. Particularly, gas-flow rate rapidly increases and reaches the maximum of 1050 m<sup>3</sup> per day at the 276<sup>th</sup> day and then follows a gentle decline. The water production rate has a rapid decrease from 2.5-0.15 m<sup>3</sup> per day after the first 273 days and then keeps gradually decreasing. The gas-water production rates of field data show high accuracy of the fractal analytical solutions.

Another comparison was implemented between the fractal analytical solution and field gas production data from the American EL PASO Exploration and Production company [16]. These gas production rate data were obtained at constant temperature. Figure 2 presents the actual field gas production rate data in the black circles and the black line for the fractal analytical solution of this paper. The analytical fractal production rate closely matches the observed gas production rate.

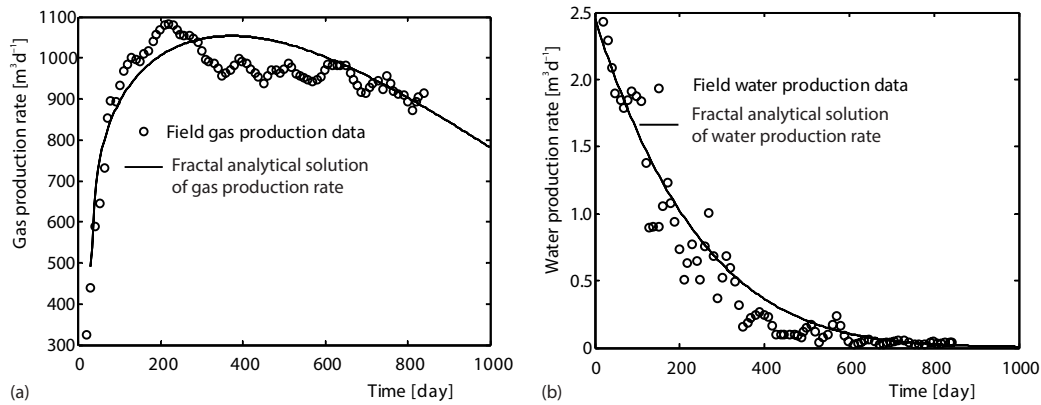


Figure 1. Comparison of fractal analytical solutions and field production rate of the gas and water in No. 1 CBM well; (a) gas production rate, (b) water production rate

## Discussion

### Impact of injection temperature

Four injection temperatures, 298 K, 317 K, 331 K, and 344 K, are assumed. The impact of injection temperature on gas production rate is presented in fig. 3. The gas production rate at the 200<sup>th</sup> day is  $1.1 \cdot 10^4$  m<sup>3</sup> per day,  $1.5 \cdot 10^4$  m<sup>3</sup> per day,  $1.8 \cdot 10^3$  m<sup>3</sup> per day, and  $1.9 \cdot 10^3$  m<sup>3</sup> per day, respectively. This figure shows that higher injection temperature corresponds to higher gas production rate. Temperature is a key parameter to control gas and heat transfer in thermal stimulation enhanced coal seam gas recovery.

### Impact of fractional order

Sensitivity analysis of this fractional order is conducted here. The fractional order is taken as 0.2, 0.35, 0.5, and 1, respectively. Figure 4 presents the gas production rate declines in the first 300 days in all the four cases. The gas production rate at the 200<sup>th</sup> day is  $2.6 \cdot 10^4$  m<sup>3</sup> per day,  $1.1 \cdot 10^4$  m<sup>3</sup> per day,  $7.0 \cdot 10^3$  m<sup>3</sup> per day and  $1.8 \cdot 10^3$  m<sup>3</sup> per day, respectively. At the 500<sup>th</sup> day, the gas production rate is  $2.3 \cdot 10^4$  m<sup>3</sup> per day,  $2.1 \cdot 10^3$  m<sup>3</sup> per day,  $5.2 \cdot 10^2$  m<sup>3</sup> per day, and  $2 \cdot 10^{-1}$  m<sup>3</sup> per day, respectively. These data show that gas production rate corresponding to larger fractional order goes down faster and reaches lower gas production rate in the production tail. The fractional order indeed affects the gas production rate.

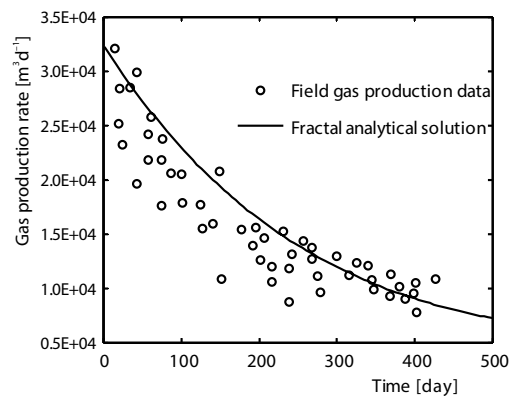


Figure 2. Model verification with field gas production rate;  $c = 0.35$  m/s,  $p_0 = 4.82$  MPa,  $k_0 = 5$  mD,  $T_0 = 298$  K,  $k_{rg} = 0.9$ ,  $k_{rw} = 0.8$

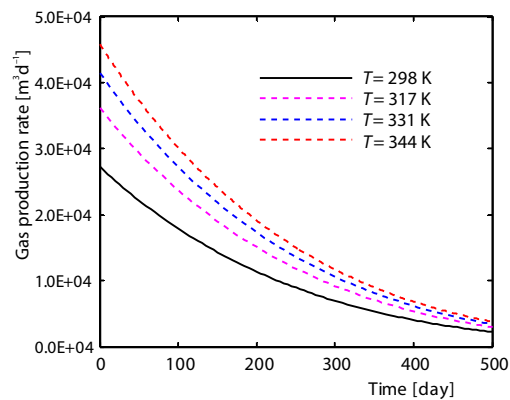
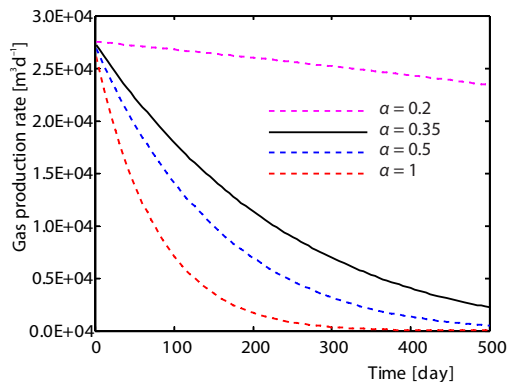


Figure 3. Impact of temperature on gas production rate



**Figure 4. Impact of fractional order on gas production rate**

analytical solutions were validated by in-situ production data, respectively. These studies can dawn the following conclusions.

- Thermal stimulation has positive impacts on the enhancement of CBM production rate in thermal stimulation enhanced gas recovery. If injection temperature is higher, the CBM production rate would decline slower and reach higher gas production rate in the production tail.
- Fractional order has a significant impact on the CBM production rate. Higher fractional order leads to a faster decline of gas production rate and a lower production rate at the same time period.

### Acknowledgment

The authors are supported by the Fundamental Research Funds for the Central Universities (Grant No. 2018BSCXC36) and Postgraduate Research & Practice Innovation Program of Jiangsu Province (Grant No. KYCX18\_1973).

### References

- [1] Wang, H., et al., Enhance Hydraulic Fractured Coalbed Methane Recovery by Thermal Stimulation, *Proceedings, Society of Petroleum Engineers*, SPE175927, Calgary, Canada, 2015
- [2] Salmachi, A., Haghighi, M., Feasibility Study of Thermally Enhanced Gas Recovery of Coal Seam Gas Reservoirs Using Geothermal Resources, *Energy Fuels*, 26 (2012), 8, pp. 5048-5059
- [3] Zhou, F., et al., Injecting Pure N<sub>2</sub> and CO<sub>2</sub> to Coal for Enhanced Coalbed Methane: Experimental Observations and Numerical Simulation, *International Journal of Coal Geology*, 116 (2013), Sept., pp. 53-62
- [4] Qu, H., et al., Complex Evolution of Coal Permeability during CO<sub>2</sub> Injection under Variable Temperatures, *International Journal of Greenhouse Gas Control*, 9 (2012), July, pp. 281-293
- [5] Lewis, R. W., et al., Finite Element Modelling of Two-Phase Heat and Fluid-Flow in Deforming Porous Media, *Transport in Porous Media*, 4 (1989), 4, pp. 319-334
- [6] Wang, J. G., Peng, Y., Numerical Modelling for the Combined Effects of Two-Phase Flow, Deformation, Gas Diffusion and CO<sub>2</sub> Sorption on Caprock Sealing Efficiency, *Journal of Geochemical Exploration*, 144 (2014), Part A, pp. 154-167
- [7] Wang, J. G., Wang, H. M., Sealing Efficiency Analysis for Shallow-Layer Caprocks in CO<sub>2</sub> Geological Storage, *Environmental Earth Sciences*, 77 (2018), Nov., 738
- [8] Teng, T., et al., A Thermally Sensitive Permeability Model for Coal-Gas Interactions Including Thermal Fracturing and Volatilization, *Journal of Natural Gas Science and Engineering*, 32 (2016), May, pp. 319-333
- [9] Shang, X. J., et al., Fractal Analysis for Heat Extraction in Geothermal System, *Thermal Science*, 21 (2017), Suppl. 1, pp. S25-S31
- [10] Teng, T., et al., Complex Thermal Coal Gas Interactions in Heat Injection Enhanced CBM Recovery, *Journal of Natural Gas Science and Engineering*, 34 (2017), Aug., pp. 1174-1190

### Conclusions

This study proposed a fractal-thermal-hydro coupling model to describe the coupling of heat conduction and two-phase flow behaviors in the process of thermal stimulation enhanced CBM recovery. A coupling equation set for two-phase flow and heat conduction was obtained in terms of local fractional time and space derivatives. This coupling equation set was analytically solved through the fractal travelling-wave method. Analytical solutions of gas pressure and gas production rate, water pressure and water production rate were obtained, respectively. The

- [11] Li, S., *et al.*, A Fully Coupled Thermal-Hydraulic-Mechanical Model with Two-Phase Flow for Coalbed Methane Extraction, *Journal of Natural Gas Science and Engineering*, 33 (2016), July, pp. 324-336
- [12] Kang, J. H., *et al.*, Numerical Modelling and Experimental Validation of Anomalous Time and Space Subdiffusion for Gas Transport in Porous Coal Matrix, *International Journal of Heat and Mass Transfer*, 100 (2016), Sept., pp. 747-757
- [13] Yang, X. J., Baleanu, D., *Local Fractional Integral Transforms and Their Applications*, Academic Press, New York, USA, 2015
- [14] Yang, X. J., *et al.*, Systems of Navier-Stokes Equations on Cantor Sets, *Mathematical Problems in Engineering*, 2013 (2013), ID 769724
- [15] Liu, H. Y., *et al.*, Fractional Calculus for Nanoscale Flow and Heat Transfer, *International Journal of Numerical Methods for Heat and Fluid-Flow*, 24 (2014), 6, pp. 1227-1250
- [16] Mora, C. A., Wattenbarger, R. A., Comparison of Computation Methods for CBM Performance, *Journal of Canadian Petroleum Technology*, 48 (2009), 4, pp. 42-48
- [17] Cao, W., *et al.*, Analysis on Coalbed Methane with Heat Injection Based on COMSOL Multiphysics, *Chinese Journal of Underground Space and Engineering*, 10 (2014), 5, pp. 1139-1145
- [18] Xue, Y. C., *et al.*, Mathematical Model Study on Gas and Water Two-Phase of Early-Time Flowback in Shale Gas Wells, *Science Technology and Engineering*, 17 (2017), 24, pp. 213-217